ANALYSIS AND DESIGN OF THE MIXING CHAMBER IN A FLAT EJECTOR

A. M. Arkhimov, M. A. Izyumov, and D. M. Khzmalyan

UDC 533.697.5

An analysis is made of the laws which govern isothermal flow in the mixing zone of an ejection chamber with a longitudinal pressure gradient. The proposed method of calculations has been verified experimentally.

Ejectors have found industrial applications. In order to design these devices, it is necessary to know the processes occurring in them and to be able to make the requisite calculations. Several studies have dealt with this problem [1-8] without considering, however, situations where the flow is supersonic or transonic. A review of these references shows two basic approaches to the design of a mixing chamber: by considering discrete sections and the use of gas-dynamic functions [1-3] or by considering continuous parameter variation on the basis of semiempirical data taken from the theory of turbulence [4-8]. The second approach seems preferable when an evaluation of the mixing process over the entire length of the chamber is required. The other approach was adopted mainly for the design of axially symmetrical ejectors with isobaric or quasiisobaric flow in the ejection zone. At the same time, many ejectors are designed so that the mixing of streams in this zone will occur under a high longitudinal pressure gradient. In order to discover the general laws and to develop a procedure for calculating such a flow mode, the authors have analyzed an ejector shown schematically in Fig. 1. The chamber dimensions, measured in nozzle diameters (b_0 = 4-10 mm), were varied as follows: $\bar{b}_c$ = 3.1-9.2, $\bar{l}_1$ = 6.8-17.0, $\bar{l}_2$ = 9-56, $\bar{B}_0$ = 2.9-9.4, $\bar{\delta}_w$ = 0.18-0.45 at a converging-channel angle α = 0-12°. The initial velocities of the ejecting and the ejected stream were U_{01} = 20-50 m/sec; U_{02} = 10-15 m/sec, respectively with $m_0 = U_{02}/U_{01}$ = 0.15-0.6 and $\rho_{01} = \rho_{02}$.

The dynamic heads and the static pressures at the transverse sections of the chamber were measured with Prandtl pneumometer tubes the diameter of which at the inlet end was 1 mm. The constancy of temperature and the initial flow rates were checked by the readings of mercury thermometers and flow meters which had been installed in the respective channels. In order to estimate the measurement error, the total flow rate was checked against the total momentum at various sections of the mixing chamber. Discrepancies in values did not exceed the permissible limits of 4-5%.

An analysis of the test data has revealed the hydrodynamic flow pattern in the ejection zone ($\bar{x} \leq \bar{x}_e$) shown in Fig. 1. The inner boundary of the mixing zone is represented by the line o–n. Depending on the hydrodynamic parameter m_0 of an ejector and on the geometry of the mixing chamber, the boundary of the mixing zone reaches the wall either behind section n–n (o–e) or before it (o–e'). Accordingly, either flow mode I or flow mode II will prevail.

The test data indicate an almost constant static pressure p(y) = const across the width of the chamber. Outside the boundary layer of the stream (n–o–e) there remain regions of undisturbed flow, to which the following relations, in terms of mean parameter values, apply at the said section:

$$p + 0.5\rho U_1^2 = p_0 + 0.5\rho U_{01}^2; \quad (1)$$

$$p + 0.5\rho U_2^2 = p_0 + 0.5\rho U_{02}^2. \quad (2)$$

The distribution of relative excess velocities within the boundary layer was found to be universal in all tests and to follow known laws [6]:

Moscow Power Institute. Translated from Inzhenerno-Fizicheskii Zhurnal, Vol. 21, No. 6, pp. 1060-1067, December, 1971. Original article submitted August 31, 1970.

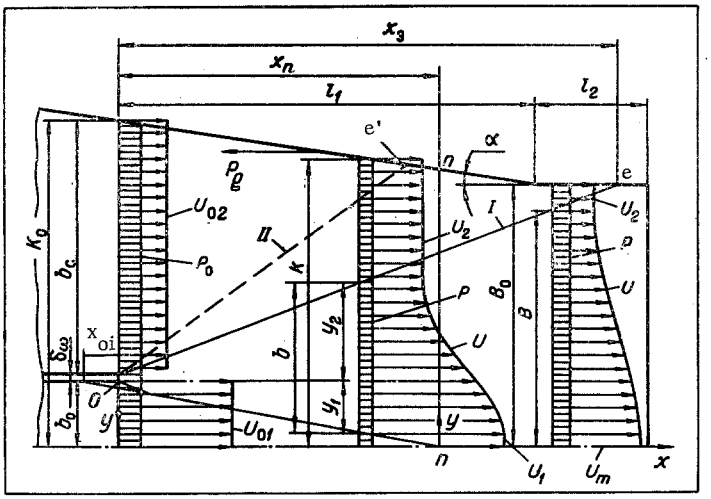

Fig. 1. Geometry of the mixing chamber and schematic representation of the flow.

$$\frac{U_1 - U}{U_1 - U_2} = (1 - \eta^{1,5})^2; \quad \eta = \frac{y - y_2}{b} = \frac{y - y_2}{y_1 - y_2} \tag{3}$$

for the initial segment and

$$\frac{U - U_2}{U_m - U_2} = (1 - \xi^{1,5})^2; \quad \xi = \frac{y}{B} \tag{4}$$

for the main segment.

The rate of mass increase in the ejecting stream (Fig. 2) can be described adequately well by the following equations:

$$G_c = [1 + 0.0362(\bar{x} - \bar{x}_{oi})]\, G_{01} = rG_{01} \tag{5}$$

for the initial segment and

$$G_c = 0.375 G_{01} \sqrt{\bar{x} - \bar{x}_{oi}} = RG_{01} \tag{6}$$

for the main segment, which confirms the conclusions in [9] concerning the universality of the ejection characteristics of jet streams. The value of $\bar{x}_{oi}$ was determined by extrapolation of the empirical lines $\bar{y}_1 = f(\bar{x})$ and $G_c - G_{01} = f_1(\bar{x})G_{01}$ to intersection with the abscissa. In all tests $\bar{x}_{oi}$ was found to be negative (with respect to the nozzle throat as reference) and equal to 1.0-3.5 in absolute value. A comparison of test data with results obtained by formulas has shown that the following equation will be satisfactory for calculating $\bar{x}_{oi}$:

$$\bar{x}_{oi} = (2\bar{b}_{ik} + 1.7\bar{b}_{iH})(1 + 2.36m_0), \tag{7}$$

which differs from the equation given in [6] by the second factor. Equation (7) has been derived using the expression for $\bar{b}(\bar{x})$ given in [9].

The reaction force P_g of a straight converging channel on the stream, when the pressure variation along the converging channel is almost parabolic (which was the case in most tests), can be approximated sufficiently well by the relation:

$$P_g = \int_{K_0}^{K} p dK = 0.5(\bar{K} - \bar{K}_0)\left[\bar{p}_0 - 0.333(a^2m^2 - m_0^2)\right] \rho U_{01}^2 b_0, \tag{8}$$

where

$$a = \frac{U_1}{U_{01}}; \quad m = \frac{U_2}{U_1}; \quad \bar{p}_0 = \frac{2p_0}{\rho U_{01}^2}; \quad \bar{K} = \frac{K}{b_0}; \quad \bar{K}_0 = \frac{K_0}{b_0}.$$

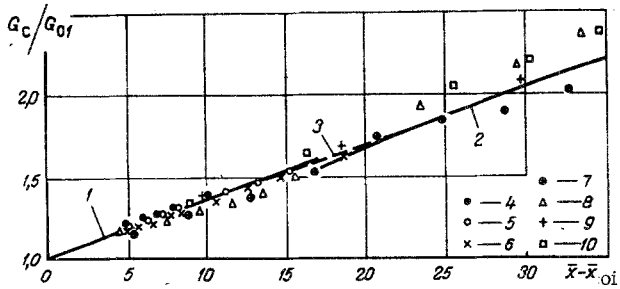

Fig. 2. Change in the stream mass: 1) calculation formula $G_c/G_{01} = 1 + 0.0362(\bar{x}-\bar{x}_{oi})$; 2) calculation formula $G_c/G_{01} = 0.375\sqrt{\bar{x}-\bar{x}_{oi}}$; 3) trend in the change of mass in the ejecting stream near the transition section. Test data: 4) $m_0 = 0.22$, $\bar{x}_{oi} = 1.9$, $\bar{p}_0 = -0.075$; 5) $m_0 = 0.42$, $\bar{x}_{oi} = -2.2$, $p_0 = 0.2$; 6) $m_0 = 0.555$, $\bar{x}_{oi} = -1.7$, $\bar{p}_0 = 0.415$; 7) $m_0 = 0.465$, $\bar{x}_{oi} = -2.0$, $\bar{p}_0 = 0.265$; for 4-7) $\bar{b}_c = 3.1$, $\bar{l}_1 = 6.8$, $\bar{l}_2 = 56$, $\bar{B}_0 = 2.9$, $\delta\omega = 0.18$; 8) $m_0 = 0.42$, $\bar{x}_{oi} = -3.5$; $p_0 = -0.04$, $\bar{b}_c = 8.22$, $\bar{K}_0 = \bar{B}_0 = 9.4$, $\delta\omega = 0.18$; 9) $m_0 = 0.195$, $x_{oi} = -1.2$; $\bar{p}_0 = 0.0$, $\bar{b}_c = 9.25$; $\bar{l}_1 = 17$, $\bar{l}_2 = 22.5$, $\delta\omega = 0.45$; 10) $m_0 = 0.195$, $\bar{x}_{oi} = -1.2$, $p_0 = -0.052$, $\bar{l}_1 = 17$, $\bar{l}_2 = 140$; $\delta\omega = 0.45$, $\bar{b}_c = 9.25$.

For practical calculations, especially when the initial segment is shorter than $\bar{l}_1$, we recommend the following formula:

$$P_g = 0.5(\bar{K} - \bar{K}_0)\left[\bar{p}_0 - 0.5(a^2m^2 - m_0^2)\right]\rho U_{01}^2 b_0, \tag{9}$$

which is not too inaccurate and which has been based on a linear pressure variation along the converging channel – as was assumed in [2]. Within the range of the geometries and the initial parameter values considered in this study, the magnitude of P_g did not exceed 30% of $\rho U_{01}^2 b_0$.

The flow formulas can be used as a basis for calculating the hydrodynamic parameters from given initial conditions. In order to simplify the calculations, we will neglect friction and the boundary layer at the wall, and also the variation in the density of the liquid due to variations in the static pressure. The calculations will be performed for a mode I flow, which is that most often encountered in the practical use of ejectors.

Initial Segment ($\bar{x} \leq \bar{x}_n$). For calculating the initial segment, we need, in addition to Eqs. (1) and (2), also equations of constant flow rate and momentum in the chamber as well as the equation of mass change in the ejecting stream:

$$U_{01}b_0 + U_{02}b_c = U_1(b_0 - b - y_2) + \int_{y_2}^{y_1} U\,dy + U_2(K - b_0 + y_2); \tag{10}$$

$$p_0K_0 + \rho U_{01}^2 b_0 + \rho U_{02}^2 b_c = \rho U_1^2(b_0 - b - y_2) + \rho\int_{y_2}^{y_1} U^2\,dy + \rho U_2^2(K - b_0 + y_2) + pK - P_g; \tag{11}$$

$$U_1(b_0 - b - y_2) + \int_{y_2}^{y_1} U\,dy = rU_{01}b_0. \tag{12}$$

After conversion to dimensionless form, with Eq. (3) and the values of the integrals taken into account, we get from Eqs. (1), (2), (10), (11), and (12):

$$\bar{p}_0 + 1 = \bar{p} + a^2; \tag{13}$$

$$\bar{p}_0 + m_0^2 = \bar{p} + a^2m^2; \tag{14}$$

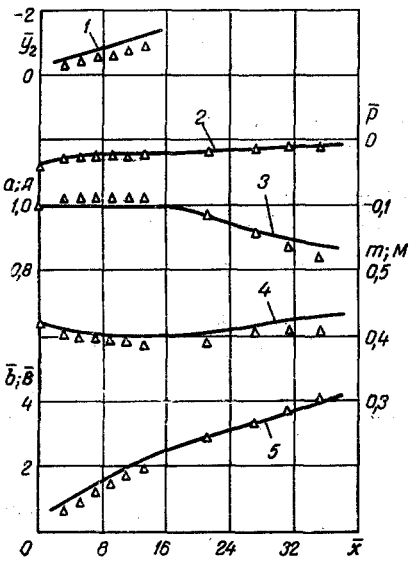

Fig. 3

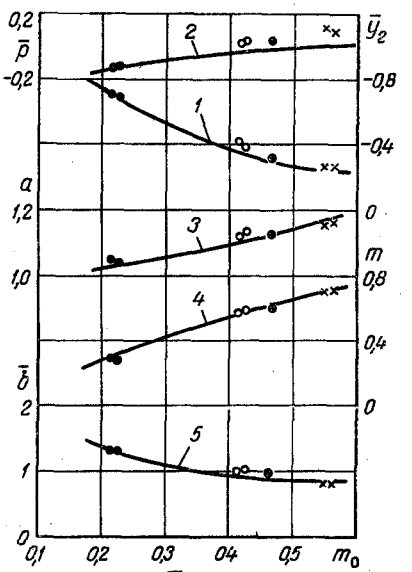

Fig. 4

Fig. 3. Flow parameters along the mixing chamber in the initial and in the main segment: calculated curve for $\bar{y}_2$ (1), for $\bar{p}$ (2), for a (A) (3), for m (M) (4), and for $\bar{b}$ ($\bar{B}$) (5); $\bar{x}_{oi}^{calc} = 3.5$, $\bar{p}_o^{calc} = \bar{p}_o^{test}$; test characteristics as in Fig. 2.

Fig. 4. Flow parameters in the initial segment ($\bar{x} = 6.8$) as a function of m_0; $\bar{x}_{oi}^{calc} = -1.1, -1.3, -1.7$, and -2.2 respectively for $m_0 = 0.2$, 0.3, 0.4, and 0.5; $\bar{p}_o^{calc} = \bar{p}_o^{test}$; symbols as in Fig. 3; test characteristics as in Fig. 2.

$$1 + m_0\bar{b}_c = a(1 - \bar{b} - \bar{y}_2) + \bar{a}\bar{b}(0.55 + 0.45m) + am(\bar{K} - 1 + \bar{y}_2); \tag{15}$$

$$1 + m_0^2\bar{b}_c + 0.5\bar{p}_0\bar{K}_0 = a^2(1 - \bar{b} - \bar{y}_2) + a^2\bar{b}(0.416 + 0.268m + 0.316m^2) + a^2m^2(\bar{K} - 1 + \bar{y}_2) + 0.5\bar{p}\bar{K} - \bar{P}_g; \tag{16}$$

$$a(1 - \bar{b} - \bar{y}_2) + \bar{a}\bar{b}(0.55 + 0.45m) = r. \tag{17}$$

Here

$$\bar{p} = \frac{2p}{\rho U_{01}^2}; \quad \bar{b} = \frac{b}{b_0}; \quad \bar{y}_2 = \frac{y_2}{b_0}; \quad \bar{P}_g = \frac{P_g}{\rho U_{01}^2 b_0}.$$

System (13)-(17) can be reduced to two equations with two unknowns ($\bar{b}$, m):

$$\bar{b} = \frac{r(1-m) + amK - \Sigma\bar{G}_0}{0.45am(1-m)}; \tag{18}$$

$$\bar{b} = \frac{m\{\Sigma\bar{I}_0 - \bar{K}[a^2 + 0.5(\bar{p}_0 + m_0^2 - a^2m^2)] + \bar{P}_g\} + a(\Sigma\bar{G}_0 - r)(1-m^2)}{a^2m(0.316m^2 + 0.268m - 0.584)}, \tag{19}$$

which admit a graphical solution. In Eqs. (18) and (19) we have: $\Sigma\bar{G}_0 = 1 + m_0\bar{b}_c$; $\Sigma\bar{I}_0 = 1 + m_0^2\bar{b}_c + 0.5\bar{p}_0\bar{K}_0$; $a = \sqrt{(1-m^2)^{-1}(1-m_0^2)}$. With $\bar{b}$, m, and a known, the flow parameters $\bar{y}_2$, $\bar{p}$, and U are determined from (13), (15), (17), and (3).

Main Segment ($\bar{x}_n \le \bar{x} \le \bar{x}_e$). Here the system which includes the conditions of mass and momentum conservation, the Bernoulli equation for the undisturbed zone of passive flow, and also the equations of mass change in the ejecting stream can be written in dimensionless form as follows:

$$\Sigma\bar{G}_0 = A\bar{B}(0.45 + 0.55M) + AM(\bar{K} - \bar{B}), \tag{20}$$

$$\Sigma\bar{I}_0 = A^2\bar{B}(0.316 + 0.268M + 0.416M^2) + A^2M^2(\bar{K} - \bar{B}) + 0.5\bar{p}\bar{K} - \bar{P}_g, \tag{21}$$

$$\bar{p}_0 + m_0^2 = \bar{p} + A^2M^2, \tag{22}$$

$$A\bar{B}(0.45 + 0.55M) = R. \tag{23}$$

Here

$$A=\frac{U_m}{U_{01}},\quad M=\frac{U_2}{U_m},\quad \bar{B}=\frac{B}{b_0},$$
$$\bar{P}_g=0.5(\bar{K}-\bar{K}_0)\left[\bar{p}_0-0.5(A^2M^2-m_0^2)\right]. \tag{24}$$

Along segment $\bar{l}_2$, where $d\bar{K}/d\bar{x}=0$, the magnitude of $\bar{P}_g$ is taken as equal to the reaction force at $\bar{x}=\bar{l}_1$. As a result of transforming (20)-(24), we obtain

$$A=\frac{R}{0.45\bar{B}}-\frac{1.22(\Sigma\bar{G}_0-R)}{\bar{K}-\bar{B}}, \tag{25}$$

$$A=\frac{-C+\sqrt{C^2-4DE}}{2D}, \tag{26}$$

which contain the sought quantities A and $\bar{B}$, while in (26) and (24)

$$C=\frac{0.268\bar{B}(\Sigma\bar{G}_0-R)}{\bar{K}-\bar{B}};\quad D=0.316\bar{B};\quad E=\left[\frac{\Sigma\bar{G}_0-R}{\bar{K}-\bar{B}}\right]^2(0.5\bar{K}-0.584\bar{B})$$
$$+0.5\bar{K}(\bar{p}_0+m_0^2)-\Sigma\bar{I}_0-\bar{P}_g;\quad A^2M^2=\left[\frac{\Sigma\bar{G}_0-R}{\bar{K}-\bar{B}}\right]^2.$$

Only the positive root in the solution to Eq. (26) for A is used, since the axial velocity cannot be negative. The system of Eqs. (25) and (26) is solved graphically. Then, M, $\bar{p}$, and U are determined from (23), (22), and (4).

Considering that $G_c=G_{01}+G_{02}$, from Eq. (6) we can find the coordinates of the flow section which corresponds to the end of the ejection zone:

$$\bar{x}_e=\frac{[\Sigma\bar{G}_0]^2}{0.141}+\bar{x}_{oi}. \tag{27}$$

If the calculated width of the boundary layer at the section having coordinate $\bar{x}_e$ at $U_{2e}=0$ remains smaller than the channel width, then the assumed flow mode I prevails in the chamber. If $\bar{B}_e$ is smaller than $\bar{B}_0$, then behind the section of coordinate $\bar{x}_e$ backstreams of the liquid will appear. The physical condition for precluding the occurrence of backstreams is that the mainstream retain its full ejection capability up to the instant when it fills the entire chamber width.

The boundary between the initial and the main segment can be determined on the basis of the relations given in [6] and [9] for the width and the inside boundary of the boundary layer during an isobaric flow of mixed streams and considering that in the transition segment $\bar{y}_1=1$:

$$\bar{x}_n=\frac{1+2.36m_0}{(3.1+m_0)\,0.0362}+\bar{x}_{oi}. \tag{28}$$

In order to determine $\bar{x}_n$ more precisely, it is necessary to plot the equations $1-\bar{y}_2=f_2(\bar{x})$ and $b=f_3(\bar{x})$ from Eqs. (13)-(19) and then to extrapolate the curves till they intersect.

Since only flow mode I is of interest in this study, we propose a method of approximately estimating the existence limits for this mode of flow. The basis of this method is, as in [7], the stipulation that the boundary layer reaches the geometrical axis and the walls of the ejector simultaneously, i.e., the condition

$$\bar{x}_n=\bar{x}_e. \tag{29}$$

Let us express $\bar{x}_e$ according to Eq. (5), taking into account that $G_c=G_{01}+G_{02}$,

$$\bar{x}_e=\frac{m_0\bar{b}_c}{0.0362}+\bar{x}_{oi}. \tag{30}$$

Equating the right-hand sides of (28) and (30), we obtain an expression relating the geometry and the hydrodynamic parameters of the ejector under condition (29):

$$\bar{b}_c=\frac{1+2.36m_0}{(3.1+m_0)\,m_0}. \tag{31}$$

If for a given m_0 ($0.15 \leq m_0 \leq 0.6$) $\bar{b}_c$ is larger than according to Eq. (31), then flow mode I prevails in the chamber; if it is smaller, then flow mode II prevails.

Since isobaric flow represents a special case in our problem, it is possible to obtain from these equations the relation $\bar{K} = f_4(\bar{x})$ which determines isobaric flow. From Eqs. (13)-(17) we have for the initial segment ($\bar{x} \leq \bar{x}_n$):

$$\bar{K} = \bar{K}_0 - \frac{0.0362(1-m_0)^2}{m_0(1+2.36m_0)}\bar{x} = \bar{K}_0 - \operatorname{tg}\alpha_{iso}\bar{x}. \tag{32}$$

If at given m_0 and $\bar{b}_c$ the angle of the converging channel is $\alpha > \alpha_{iso}$, then in the initial segment the velocities am, a increase while the pressure decreases. The converse holds for $\alpha < \alpha_{iso}$. The longitudinal gradients of the other flow parameters depend on the manner in which am and a vary. The condition of isobaric flow in the main segment ($\bar{x}_n \leq \bar{x} \leq \bar{x}_e$) is obtained from Eqs. (20)-(23):

$$\bar{K} = \frac{\Sigma\bar{G}_0 - R}{m_0} + \frac{c - \sqrt{c^2 - 4de}}{2d}, \tag{33}$$

where

$$c = 1 - m_0(1 - 2.12R); \quad d = 0.559m_0^2; \quad e = 1.56R^2.$$

Only the negative square root is used in Eq. (33), since otherwise $\bar{K} > \bar{K}_0$ and this is incompatible with the condition of isobaric flow.

For illustration, experimental data and calculated distributions of the flow parameters along the $\bar{x}$-axis in the initial and in the main segment of the ejector are shown in Fig. 3. Experimental and theoretical values of the flow parameters for the initial segment at a fixed distance $\bar{x}$ are shown in Fig. 4. The agreement between calculated and tested results in both Fig. 3 and Fig. 4 may be considered close enough.

LITERATURE CITED

1. G. N. Abramovich, Applied Gas Dynamics [in Russian], Nauka (1969).
2. E. Ya. Sokolov and N. M. Zinger, Jet Devices [in Russian], Gosénergoizdat (1960).
3. A. P. Kovalev, Ya. A. Kagan, and D. M. Khzmalyan, Design of Ejectors for Furnaces in Boiler Rooms [in Russian], Teploénergetika, No. 9 (1963).
4. P. N. Romanenko, "Theory of ejection and the design of jet devices," Izv. Akad. Nauk SSSR, Otd. Tekh. Nauk, No. 6 (1953).
5. M. V. Polikovskii, "Designing the inlet stage of an ejector," Izv. Akad. Nauk SSSR, Otd. Tekh. Nauk, No. 1 (1957).
6. G. N. Abramovich, Theory of Turbulent Streams [in Russian], Fizmatgiz (1960).
7. O. V. Yakovlevskii, in: Analysis of Turbulent Air, Plasma, and Real-Gas Streams [in Russian], Mashinostroenie (1967).
8. R. Vasudevan, Author's Abstract of Candidate's Dissertation [in Russian], Moscow Power Institute (1967).
9. O. V. Yakovlevskii, Izv. Akad. Nauk SSSR, Otd. Tekh. Nauk, No. 3 (1961).